Geometrical and Mechanical Properties of Large Rolled Steel Angles

MURTY K.S. MADUGULA, TOSHIFUMI KOJIMA, YASUYUKI KAJITA, AND MICHIHIRO OHAMA

ABSTRACT

Steel angles are the most frequently used sections in electrical transmission towers. To carry safely the heavy leg loads of 500 kV towers, N. K. K. Corporation, Japan, developed the world's largest rolled steel angles (300 × 300 × 35 and 350 × 350 × 35 mm size). The paper describes the manufacturing process and presents the geometrical properties. The statistical analysis of samples over a three-year period showed that the steel used is consistently of uniform quality. Based on 12 tensile tests of round specimens in as-supplied condition and another 12 specimens in heat-treated condition carried out at 20°C, -20°C, –40°C, and –65°C, it was concluded that decrease of temperature did not result in any decrease in elongation and only three percent decrease in the reduction of area. Due to heat-treatment, the maximum reduction in yield stress and tensile strength was two percent, maximum reduction in elongation three percent, and maximum reduction of area two percent.

1. INTRODUCTION

Steel angles are the most frequently used shapes in latticed electrical transmission towers and communication towers, because of the ease of their fabrication, transportation, and erection. But, for extra-high-voltage electrical transmission towers (500 kV towers) and tall communication towers (over 200 m in height), the leg loads will be higher than the load-carrying capacity of the heaviest rolled-steel angle section (250 × 250 × 25 mm). In such a case, either welded steel angle sections, solid rounds, or round hollow structural sections are used, which increases significantly the cost of these towers. Therefore, N. K. K. Corporation, Japan, has developed the world's largest rolled steel angles—300 × 300 × 35 and 350 × 350 × 35 mm size.

Murty K.S. Madugula is professor, department of civil and environmental engineering, University of Windsor, Windsor, Ontario, Canada

Toshifumi Kojima is senior research engineer, Keihin Research Department, Materials and Processing Research Center, N. K. K. Corporation, Kawasaki, Japan

Yasuyuki Kajita is engineer, plate department, plate mill, Fukuyama Works, N. K. K. Corporation, Fukuyama, Japan

Michihiro Ohama is manager, product design and quality control, rail and section, Fukuyama Works, N. K. K. Corporation, Fukuyama, Japan

2. MANUFACTURING PROCESS

Molten iron from the blast furnace is first desulfurized. Steel is made in a basic oxygen furnace with combined top and bottom blowing (oxygen from the top and carbon dioxide, argon, and nitrogen from the bottom through a multiple hole plug) to homogenize the molten bath. The molten steel from the basic oxygen furnace goes through a secondary refining process, which includes alloy addition, dephosphorization, further desulfurization, deoxidization, degassing (removal of hydrogen and other gases from the molten steel to produce a "clean" steel product), and constituent adjustment. After degassing, slabs 220 × 675 mm are cast in a continuous casting machine. The advantages of continuous casting are:

a. "cleanliness" of slab
b. homogenization of texture by uniform cooling, and
c. smooth appearance of the slab surface.

These slabs are charged into a reheating furnace for hot rolling using four two-high angle-rolling mills. After cooling, all angles are roller-straightened (four upper and five lower rolls) and, if necessary, are passed through a gag press to meet the specification limits for camber and sweep. The schematic of the manufacturing process is shown in Figure 1.

The steel is produced to Japanese Industrial Standard Specification (1987) JIS G3101—Class SS 540 (i.e., minimum tensile strength is 540 MPa). The uniformity of chemical composition and mechanical properties can be seen from the results of the statistical analysis presented in Tables 1(a) and 1(b). The rolling process produces angles whose variation in cross-sectional dimensions [given in Tables 1(c) and 1(d)] is well within the specification limits of the Japanese Industrial Standard Specification (1990) JIS G3192. The samples were taken from a total production of 2,800 tons over a period of three years ending December 1993.

3. GEOMETRICAL PROPERTIES

The geometrical properties of the two sizes of angles are given in Table 2. The fillet, toe, and heel radii—r_1, r_2, and r_3, respectively, are identified in Figure 2. In addition to the usual

Table 1a. Results of Statistical Analysis of Chemical Composition (Mass %)						
	C	Si	Mn	P	S	V
Number of Samples	14	14	14	14	14	14
Average	0.163	0.201	1.44	0.012	0.0023	0.049
Standard Dev.	0.005	0.006	0.002	0.003	0.0012	0.003
Specification LImits (JIS G3101—Class SS 540 (1987)	0.30 max	—	1.60 max	0.040 max	0.040 max	—

Table 1b. Results of Statistical Analysis of Mechanical Properties						
	300 × 300 × 35 mm			350 × 350 × 35 mm		
Angle Size	Yield Stress (MPa)	Tensile Strength (MPa)	Elong. 200 mm G.L. (%)	Yield Stress (MPa)	Tensile Strength (MPa)	Elong. 200 mm G.L. (%)
Number of Samples	33	33	33	30	30	30
Average	477	613	26.5	474	617	25.5
Standard Deviation	16	11	2.0	17	17	2.3
Spec. Limits JIS G 3101—Class SS 540 (1987)	390 min.	540 min.	17 min.	390 min.	540 min.	17 min.
Note: G.L. = gage length						

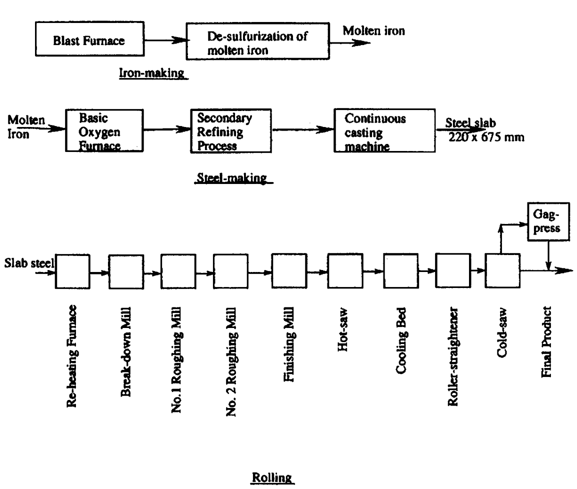

Fig. 1. Schematic of the manufacturing process.

fillet and toe radii, these angles are provided with a heel radius of 10 mm, which serves the following two purposes:

a. Elimination of the need for grinding of the heel to facilitate splicing, thus making splicing economical, and
b. Bringing the extreme fiber closer to the minor axis, thus increasing the minor axis elastic section modulus, S_z.

All cross-sectional properties, except Saint-Venant torsion constant J, are computed taking into account the fillet, toe, and heel radii. The values are rounded off to three significant figures, as per the usual practice.

Because the angle sections are torsionally weak, they are susceptible to flexural-torsional buckling and lateral-torsional buckling, and it will be necessary to compute the warping constant C_w and the torsion constant J, for use in strength calculations.

The warping constant C_w is computed using Equation 1 given in Bleich (1952):

$$C_w = (\text{Area})^3 / 144 \tag{1}$$

Table 1c.
Variation in Sectional Dimensions (mm)
(for 300 × 300 × 35 mm)

Angle Size	300 × 300 × 35 mm				
	Leg width	**Thickness**	**Camber[1]**	**Sweep[2]**	**Out-of-Square**
Number of samples	50	50	25	25	25
Average	300.1	35.1	3.2	4.3	0.5
Standard Deviation	0.53	0.36	1.14	1.62	0.98
Spec. Limits JIS G 3192 (1990)	±4.0	±1.5	0.30% of L max. (= 30 mm)	0.30% of L max. (= 30 mm)	2.5% of leg width max. (= 7.5 mm)

Notes:
1. Camber is the out-of-straightness of the heel in the plane of symmetry. The length of the specimen is 10 m.
2. Sweep is the out-of-straightness of the toe in the plane perpendicular to the plane of symmetry. The length of the specimen is 10 m.

Table 1d.
Variation in Sectional Dimensions (mm)
(for 350 × 350 × 35 mm)

Angle Size	350 × 350 × 35 mm				
	Leg width	**Thickness**	**Camber[1]**	**Sweep[2]**	**Out-of-Square**
Number of samples	50	50	25	25	25
Average	349.3	35.2	3.2	4.0	0.7
Standard Deviation	0.52	0.38	1.72	1.54	0.95
Spec. Limits JIS G 3192 (1990)	±4.0	±1.5	0.30% of L max. (= 30 mm)	0.30% of L max. (= 30 mm)	2.5% of leg width max. (= 8.75 mm)

Notes:
1. Camber is the out-of-straightness of the heel in the plane of symmetry. The length of the specimen is 10 m.
2. Sweep is the out-of-straightness of the toe in the plane perpendicular to the plane of symmetry. The length of the specimen is 10 m.

The torsion constant J is calculated from the following expression, which includes the effect of fillet radius (El-Darwish and Johnston, 1965):

$$J = (1/3) \times (\text{Centerline Length}) \times t^3 + C \times D^4 - 0.315 \times t^4 \quad (2)$$

in which the juncture diameter parameter

$$D = 0.343r_1 + 1.172t \quad (3a)$$

and the juncture coefficient

$$C = 0.0728 + 0.0571 \times (r_1 / t) - 0.0049 \times (r_1 / t)^2 \quad (3b)$$

where, r_1 = radius of fillet, and t = thickness of the leg of the angle.

4. MECHANICAL PROPERTIES

(a) Objectives

The present investigation is aimed at supplementing the existing test data on these angles and has the following objectives:

(i) To determine the tensile and compressive stress-strain characteristics of the material from tests on rectangular specimens (with thickness equal to the thickness of the angle leg)

Table 2. Geometrical Properties		
Size of angle (mm)	300 × 300 × 35	350 × 350 × 35
Fillet radius, r_1 (mm)	24	24
Toe radius, r_2 (mm)	18	18
Heel radius, r_3 (mm)	10	10
Cross-sectional area, A (mm^2)	19,700	23,200
Mass (kg/m)	155	182
Centroid, $\bar{x}$, $\bar{y}$ (mm)	87.1	99.6
Moment of inertia, I_x, I_y (10^6 mm^4)	163	266
Max. moment of inertia, I_w (10^6 mm^4)	259	423
Min. moment of inertia, I_z (10^6 mm^4)	66.9	108
Product of inertia, I_{xy} (10^6 mm^4)	96.0	158
Radius of gyration, r_x, r_y (mm)	90.9	107
Max. radius of gyration, r_w (mm)	115	135
Min. radius of gyration, r_z (mm)	58.2	68.3
Elastic section modulus, S_x, S_y (10^3 mm^3)	766	1,060
Max. elastic section modulus, S_w (10^3 mm^3)	1,220	1,710
Min. elastic section modulus, S_z (10^3 mm^3)	562	790
Plastic section modulus, Z_x, Z_y (10^3 mm^3)	1,390	1,930
Max. plastic section modulus, Z_w (10^3 mm^3)	1,950	2,710
Min. plastic section modulus, Z_z (10^3 mm^3)	991	1,370
Warping constant, C_w (10^9 mm^6)	53.4	87.1
Torsion constant, J (10^6 mm^4)	8.25	9.68

for use at a later date in establishing the compressive, bending, and tensile resistances of these angles.

(ii) To investigate the effect of heat treatment and low temperature on the tensile stress-strain characteristics. This information will be useful to study the suitability of these angles for use as members in structures which are prone to brittle fracture (such as bridges) where low-temperature notch toughness is a requirement. It is realized that these stress-strain curves will indicate the behavior of small smooth specimens only and are not indicative of the behavior of specimens with stress-raisers. The study of the behavior of notched specimens at low temperatures is the subject of a separate paper, which includes fracture mechanics considerations.

(b) Details of Tests

(i) Tensile Test on a Rectangular Specimen

A standard rectangular tensile test specimen (nominal width = 40 mm and thickness = full thickness of angle leg) was tested in a 2 MN capacity universal testing machine. The location of the coupon from which the test specimen was machined is shown in Figure 3. Strain readings were obtained from electrical resistance strain gages (5 mm gage length and 100,000 micro-strain range). The resulting stress-strain curve from the load-strain diagram obtained by an autographic recording device is shown in Figure 4(a), where the upper yield stress and the lower yield stress can be clearly seen. The behavior was elastic-perfectly plastic up to a strain of 0.012, when strain-hardening began. The data obtained from this test is presented in Table 3.

Table 3. Mechanical Properties Obtained from Rectangular Test Specimens					
Type of Test	**Upper Yield Stress (MPa)**	**Lower Yield Stress (MPa)**	**Strain at the beginning of strain hardening**	**E_s at 2% strain (MPa)**	**E_s at 3% strain (MPa)**
Tensile Test	485	458	0.012	4,600	3,200
Compressive Test	490	462	0.012	5,800	5,000
Note: E_S is the strain hardening modulus.					

(ii) Compressive Test on a Rectangular Specimen

A rectangular prismatic test specimen (from coupon located next to the tensile test coupon as shown in Figure 3) of length equal to four times the thickness with carefully machined parallel sides and ends (actual dimensions after machining—40.02 mm wide, 32.99 mm thick, and 139.81 mm long), was subjected to axial compressive loading in a 2 MN capacity universal testing machine (the same machine used for tensile testing). As is the case for the tensile test, strain readings were obtained from 5 mm gage length, 100,000 microstrain range electrical resistance strain gages, and the resulting stress-strain curve from the load-strain diagram obtained by an autographic recording device is shown in Figure 4(b), and the data is given in Table 3.

(iii) Low -Temperature Tests

To study the effect of low temperature and galvanizing on the yield stress, tensile strength, elongation, and reduction of area, tensile tests were carried out on a total of 24 test specimens (12.5 mm diameter, 50 mm gage length) at temperatures of 20°C, –20°C, –40°C, and –65°C.

To study the effect of galvanizing on the mechanical properties, a portion of the leg of a 300 × 300 × 35 mm angle was cut and kept in a furnace (maintained at 470°C) for 400 seconds and air-cooled. Though the duration of dipping of members of a structure in a galvanizing bath is generally 150 seconds or less, since the test pieces were to be machined from the center of the thickness of leg, the duration of heat-treatment was kept at 400 seconds.

The location of the coupons from which the test specimens were machined and their designation is shown in Figure 3, while the specimen identification numbers and the corresponding test temperatures are given in Table 4.

For low-temperature testing, the test specimens were enclosed in a cylindrical cooling chamber (coolant: liquid nitrogen + air) and the specified temperature was maintained for 15 minutes, before proceeding with the testing in a 100 kN tensile testing machine. The testing was carried out with the specimens inside the cooling chamber at the specified temperature. Figure 5 shows the testing machine and the cooling chamber (with the specimen inside). The speed of the cross-head was maintained at 5 mm/min. throughout the test. Elongation during the test was monitored by a transducer with a range of 10 mm (equal to 20 per cent elongation over a gage length of 50 mm) and load versus elongation was directly plotted by an autographic recording device. After fracture, the final length and diameter were measured with a laser micrometer (direct digital reading to 0.005 mm). Typical stress-strain curves (obtained from the load-elongation curves) at the four test temperatures for as-supplied specimens (A-1 to A-4) are shown in Figure 6(a) and for heat-treated specimens (D-1 to D-4) in Figure 6(b).

Yield stress, tensile strength, elongation, reduction of area, strain at the beginning of strain-hardening, and strain at

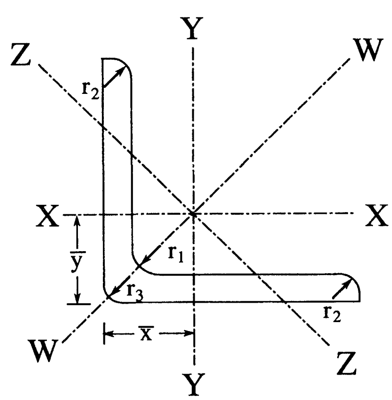

Fig. 2. Identification of axes and notation.

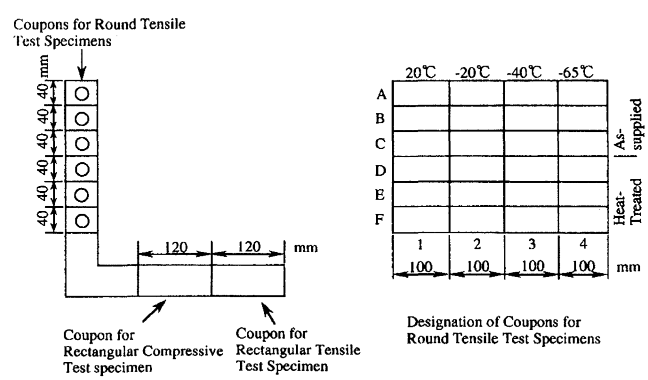

Fig. 3. Location of coupons for test specimens.

Table 4.
Specimen Designation for Low-Temperature Tests
Specimen size: 12.5 mm diameter, gage length = 50 mm

Specimen condition	Specimen Designation	Test Temperature, °C
As supplied	A-1, B-1, C-1	20
	A-2, B-2, C-2	–20
	A-3, B-3, C-3	–40
	A-4, B-4, C-4	–65
Heat treated (470°C for 400 seconds)	D-1, E-1, F-1	20
	D-2, E-2, F-2	–20
	D-3, E-3, F-3	–40
	D-4, E-4, F-4	–65

maximum stress are presented in Table 5(a) for as-supplied specimens and in Table 5(b) for heat-treated specimens. The increase in the yield stress and tensile strength due to decrease in temperature is shown in Tables 6(a) and 6(b) and Figure 7. The increase in yield stress can be predicted with reasonable accuracy using the following formula (Japan Welding Engineering Society, 1975):

$$YS = YS_0 \times \exp[329.6 - 66.5 \ln (YS_0) \times (T^{-1} - 293^{-1})] \quad (4a)$$

where

YS = predicted yield stress (kgf / mm^2) at any temperature T (°K) less than the room temperature of 293°K

YS_0 = yield stress of the material (kgf / mm^2) at the room temperature of 293°K

In the SI system of units,

$$YS = YS_0 \times \exp[481.4 - 66.5 \ln (YS_0) \times (T^{-1} - 293^{-1})] \quad (4b)$$

where

YS = predicted yield stress (MPa) at any temperature T (°K) less than the room temperature of 293°K

YS_0 = yield stress of the material (MPa) at the room temperature of 293°K, and

T = Temperature (°K) less than 293°K at which the yield stress is required to be predicted

The predicted ratios at –20°C, –40°C, and –65°C, using Equation 4(b), are also shown in Tables 6(a) and 6(b) and it can be readily seen that the agreement between the test results and the predicted values is quite satisfactory.

Decrease of temperature did not result in any decrease in elongation and resulted in only less than three percent decrease in the reduction of area. All failures were of the ductile

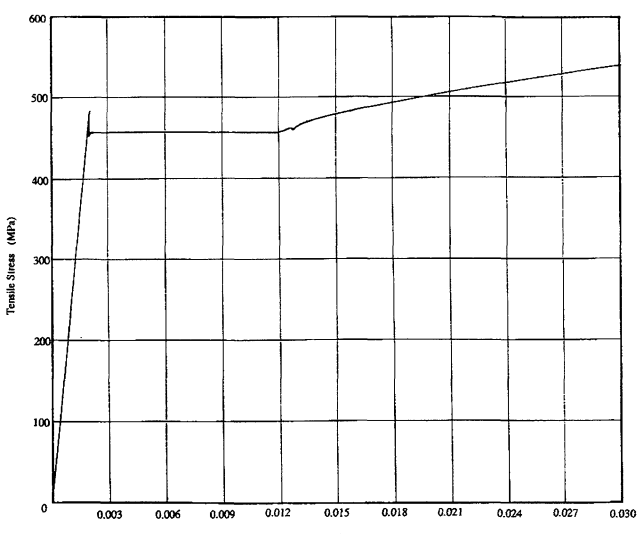

Fig. 4a. Tensile stress-strain curve (rectangular test specimen).

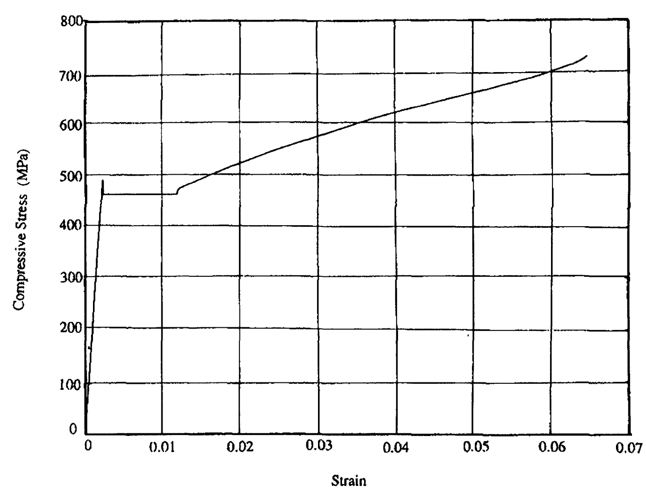

Fig. 4b. Compressive stress-strain curve (rectangular test specimen).

Table 5a. Tensile Test Results for As-Supplied Specimens							
Temp. (T°C)	Specimen No.	Yield Stress (MPa)	T.S. (MPa)	Elong. (%)	Reduction of area (%)	Strain at the beginning of strain hardening	Strain at max. stress
20	A-1	462	619	32	72	0.016	0.13
	B-1	454	626	31	70	0.013	0.14
	C-1	452	627	29	69	0.010	0.13
	Ave.	456	624	31	70	0.013	0.13
–20	A-2	477	646	31	72	0.018	0.14
	B-2	478	654	30	70	0.011	0.13
	C-2	475	654	30	69	0.014	0.14
	Ave.	476	651	31	70	0.014	0.13
–40	A-3	497	658	32	70	0.018	0.14
	B-3	488	666	31	70	0.014	0.14
	C-3	489	669	31	69	0.015	0.14
	Ave.	492	664	31	70	0.016	0.14
–65	A-4	523	684	33	71	0.022	0.14
	B-4	522	691	31	68	0.014	0.13
	C-4	516	688	30	66	0.015	0.13
	Ave.	520	688	31	68	0.017	0.13

Note: T.S. = Tensile Strength.

type. Comparing Tables 5(a) and 5(b), it can be seen that the maximum reduction in yield stress and tensile strength due to heat treatment was only two percent.

From the 24 tensile stress-strain curves, the values of strain-hardening modulus E_s were computed for strains between 0.02 and 0.08 at intervals of 0.01. It was found that the effect of temperature as well as heat treatment on E_s was negligible. Therefore, the average values of strain-hardening modulus E_s obtained from the 24 curves are plotted in Figure 8.

5. CONCLUSIONS

From the statistical analysis of samples over a period of three years, and the experimental investigation reported herein, the following conclusions can be drawn:

1. Steel used in the rolling of the angles is consistently of uniform quality. Thus, it may be possible to use a higher value for the resistance factor ϕ in the Load and Resistance Factor Design (Limit States Design) for the same reliability ('Beta' factor). (The resistance factor takes into account the possible variations in the geometrical properties as well as material properties).
2. The variation in the cross-sectional dimensions are well within the specification limits.
3. The material is elastic-perfectly-plastic up to 0.012

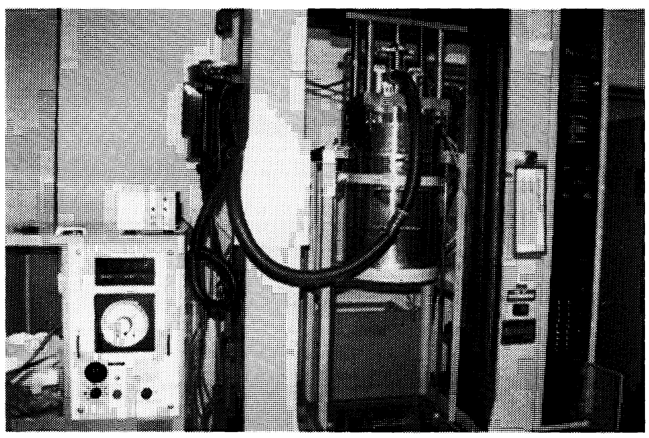

Fig. 5. Low-temperature tensile tests.

Table 5b.
Tensile Test Results for Heat-Treated Specimens

Temp. (T°C)	Specimen No.	Yield Stress (MPa)	T.S. (MPa)	Elong. (%)	Reduction of area (%)	Strain when strain hardening begins	Strain at max. stress
20	D-1	451	625	29	68	0.010	0.12
	E-1	446	620	30	69	0.012	0.13
	F-1	442	617	29	68	0.010	0.12
	Ave.	447	620	29	69	0.010	0.12
−20	D-2	473	652	28	68	0.012	0.13
	E-2	469	650	28	70	0.013	0.13
	F-2	462	641	26	70	0.012	0.13
	Ave.	468	648	28	69	0.012	0.13
−40	D-3	490	670	31	68	0.014	0.14
	E-3	487	665	28	69	0.014	0.13
	F-3	475	664	29	69	0.011	0.12
	Ave.	484	666	29	69	0.013	0.13
−65	D-4	520	691	31	66	0.014	0.14
	E-4	521	690	29	66	0.016	0.13
	F-4	516	687	31	68	0.015	0.13
	Ave.	519	690	30	67	0.015	0.13

Note: T.S. = Tensile Strength.

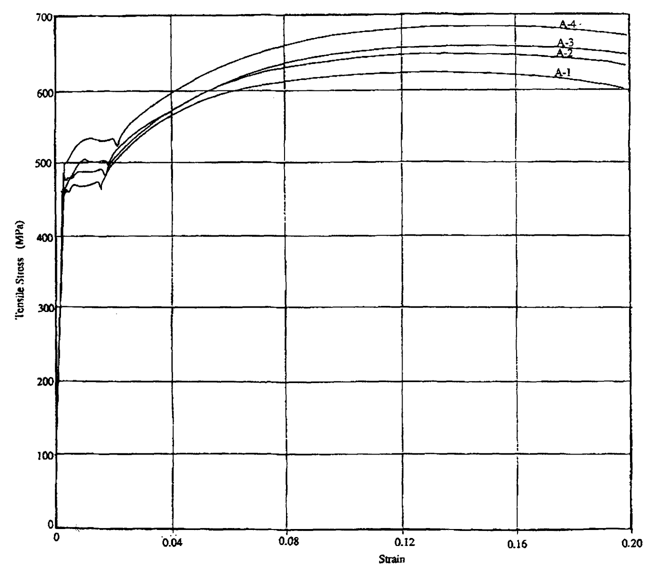

Fig. 6a. Typical stress-strain curves for as-supplied specimens.

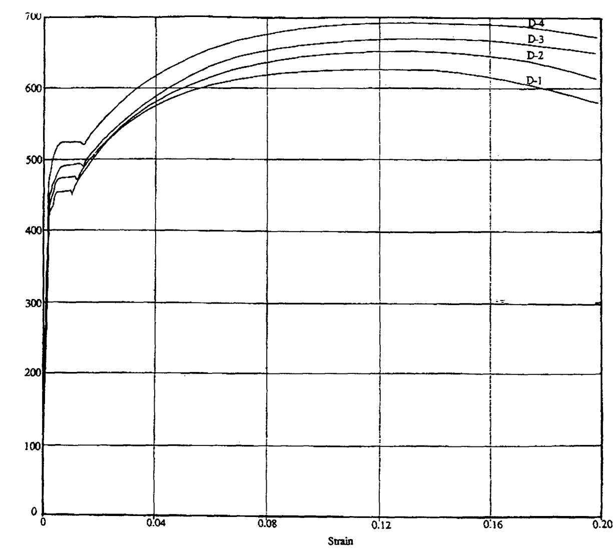

Fig. 6b. Typical stress-strain curves for heat-treated specimens.

strain. It has distinct upper-yield stress and lower-yield stress, and has a low yield ratio (the ratio of yield stress to tensile strength), which is highly desirable.

4. The yield stress and the tensile strength increase at a greater rate with decrease of temperature and can be predicted with reasonable accuracy by the equation given in the Japan Welding Engineering Society Steel Division Technical Committee Cooperative Research Report (1975). Decrease in temperature did not result in any decrease in elongation and resulted in only less than three percent decrease in reduction of area. There is thus no loss of ductility (no brittle fracture) with decrease in temperature for round smooth specimens up to at least −65°C.
5. Due to heat-treatment, maximum reduction in yield stress and tensile strength is two percent; maximum reduction in elongation is three percent, and reduction of area is two percent.
6. With the decrease of temperature, the onset of strain hardening is delayed (e.g., 0.013 strain at 20°C and 0.017 strain at −65°C).
7. Heat treatment (470°C for 400 s) advanced the initiation of strain hardening (maximum difference 0.003 strain); maximum stress is also attained at 0.01 lesser strain.
8. The effect of temperature and heat-treatment on the strain hardening modulus is negligible.

6. ACKNOWLEDGEMENT

The first author gratefully acknowledges the financial support provided by N. K. K. Corporation, Tokyo, Japan, for carrying out this investigation.

7. REFERENCES

Bleich, F., *Buckling Strength of Metal Structures*, McGraw-Hill Book Company Inc., New York, N.Y., 1952, p. 120.

El-Darwish, I. A. and Johnston, B. G., "Torsion of Structural Shapes," *Journal of the Structural Division*, Proceedings of the American Society of Civil Engineers, Vol. 91, No. STI, 1965, pp. 203–227.

Japan Welding Engineering Society, *Steel Division Technical Committee Cooperative Research Report*, Japan Welding Engineering Society (in Japanese), 1975.

Japanese Standards Association, *Rolled Steel for General Structure*, Japanese Standards Association, JIS G3101, Tokyo, Japan, 1987.

Japanese Standards Association, *Dimensions, Weight, and Permissible Variation of Hot-Rolled Steel Sections*, Japanese Standards Association, JIS G3192, Tokyo, Japan, 1990.

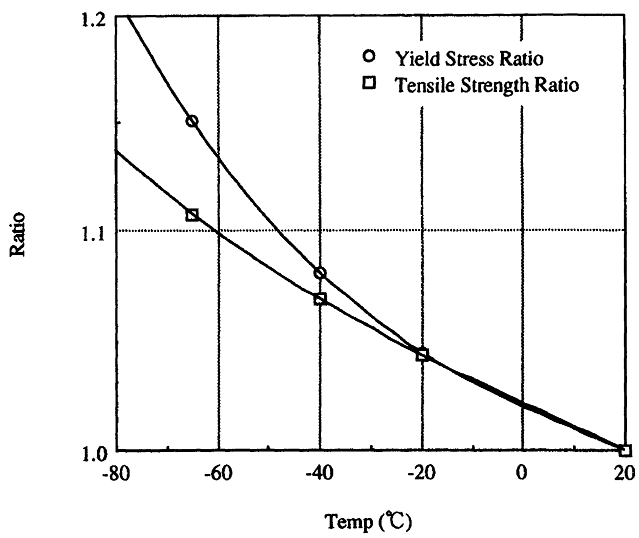

Fig. 7. Effect of temperature on the yield stress and tensile strength.

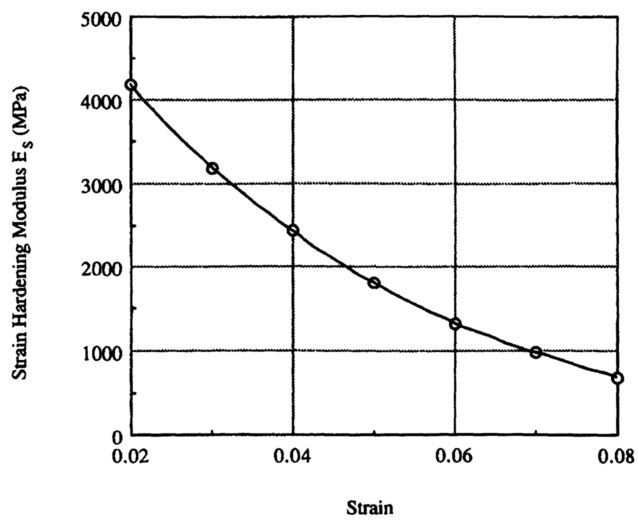

Fig. 8. Variation of E_S with respect to strain.

Table 6a. Effect of Temperature on the Yield Stress and the Tensile Strength for As-Supplied Specimens					
		Ratio of Y.S. at T°C to Y.S. at 20°C			
Temp. (T°C)	Ave. Yield Stress (MPa)	Test	Predicted Eq. 4(b)	Ave. Tensile Strength (MPa)	Ratio of T.S. at T°C to T.S. at 20°C
20	456	1.00	1.00	624	1.00
–20	476	1.04	1.04	651	1.04
–40	492	1.08	1.07	664	1.06
–65	520	1.14	1.11	688	1.10

Note: Y.S. = Yield Stress; T.S. = Tensile Strength.

Table 6b. Effect of Temperature on the Yield Stress and the Tensile Strength for Heat-Treated Specimens					
		Ratio of Y.S. at T°C to Y.S. at 20°C			
Temp. (T°C)	Ave. Yield Stress (MPa)	Test	Predicted Eq. 4(b)	Ave. Tensile Strength (MPa)	Ratio of T.S. at T°C to T.S. at 20°C
20	447	1.00	1.00	620	1.00
–20	468	1.05	1.04	648	1.05
–40	484	1.08	1.07	666	1.07
–65	519	1.16	1.11	690	1.11

Note: Y.S. = Yield Stress; T.S. = Tensile Strength.